Equation of state of hexagonal closed packed iron under Earth's core conditions from quantum Monte Carlo calculations

E. Sola,[1,2] J. P. Brodholt,[1,2] and D. Alfè[1,2,3,4]
[1]*Department of Earth Sciences, University College London, Gower Street, London WC1E 6BT, United Kingdom*
[2]*Materials Simulation Laboratory, University College London, Gower Street, London WC1E 6BT, United Kingdom*
[3]*Department of Physics and Astronomy, University College London, Gower Street, London WC1E 6BT, United Kingdom*
[4]*London Centre for Nanotechnology, University College London, 17-19 Gordon Street, London WC1H 0AH, United Kingdom*
(Received 4 November 2008; revised manuscript received 11 December 2008; published 13 January 2009)

We applied quantum Monte Carlo techniques to compute the equation of state of hexagonal closed packed iron in the range of pressure relevant to Earth's core. We used an accurate iron pseudopotential with a frozen Ne core. Trial wave functions have been obtained from density-functional theory (DFT) plane-wave calculations and expanded in systematically improvable *B* splines. Tests with various exchange-correlation functionals showed that the B3LYP functional is the one that provided the best trial wave functions. Diffusion Monte Carlo calculations were carried out using simulation cells with up to 96 atoms (1536 electrons), with some attempts to use up to 150 atoms, and corrected for finite-size errors using the scheme of Chiesa *et al.* [Phys. Rev. Lett. **97**, 076404 (2006)] and Kwee *et al.* [Phys. Rev. Lett. **100**, 126404 (2008)]. The calculated equation of state agrees closely with the experiments of Mao *et al.* [J. Geophys. Res. **95**, 21737 (1990)] and those of Dewaele *et al.* [Phys. Rev. Lett. **97**, 215504 (2006)]. It also agrees with the DFT data of Söderlind *et al.* [Phys. Rev. B **53**, 14063 (1996)] and Alfè *et al.* [Phys. Rev. B **61**, 132 (2000)], and therefore, reinforces those previous calculations.

DOI: 10.1103/PhysRevB.79.024107 PACS number(s): 64.30.Ef, 71.15.−m, 71.10.−w

I. INTRODUCTION

Many studies on iron under high pressures have been published in the last decades.[1–22] The interest in this system has its origin on the fact that iron is the main constituent of Earth's core, and therefore knowledge of its thermodynamic properties under high pressure and high temperature is of great importance to our understanding of Earth's deep interior. Several groups have experimentally measured the room-temperature equation of state (EOS) of hexagonal close packed (hcp) iron at pressures ranging from 16 up to 300 GPa.[1,2] However, at Earth's core conditions iron is subjected not just to high pressure but also to high temperatures ranging from ~4000 at the top of the core to over ~6000 K at the center of the planet. Performing experiments under these extreme conditions is challenging, and yet they are important to understand the properties of Earth's interior.

A long-standing controversy on the physics of iron at Earth's core conditions is its melting curve. This is a particularly interesting property because at a depth of 5125 km the outer liquid core freezes, and therefore at the boundary between the outer core and the solid inner (the ICB) the temperature must be the liquidus temperature of what the core is made of. Since over 90% of the core is made of Fe, its melting temperature at the pressure of the ICB gives a close estimate of the temperature of the Earth at that depth. This idea has been exploited for over 20 years, with a number of experimental groups trying to measure the high-pressure melting curve of Fe. Two main classes of experimental techniques exist: (i) static high-pressure experiments performed using diamond-anvil cells (DACs), where the sample is embedded in a pressure medium and compressed between two anvils made of diamond, and (ii) shock wave (SW) experiments, where a high velocity impactor (with a speed of the order of ~5–10 km/s) is fired at the sample, and upon impact it generates high pressure and increases the temperature of the sample. Fast optics are used to follow the behavior of the shock wave which propagates inside the sample. In DAC experiments the sample can be heated by lasers shone through the diamonds, and the temperature can be measured using pyrometric techniques. Melting of the sample is usually detected by visual inspection or by x-ray spectroscopy. SW experiments naturally provide a typical pressure vs volume curve known as the Hugoniot, which is the locus of points satisfying the Rankine-Hugoniot relation.[23] Information is extracted by measuring the speed of the shock, which depends on the speed of the impactor and the physical properties of the target. In particular, the onset of melting can be easily detected by the appearance of a discontinuity in the speed of sound of the sample. Temperature is not usually measured in SW experiments but is deduced by integrating the appropriate thermodynamic equation using estimates for the specific heat and the Grüneisen parameter.[9]

Because of the extreme conditions of pressures and temperatures, it is not surprising that different groups reported significantly different melting points.[5–10] An alternative approach followed by us[13–15] and others[16,17] was to calculate the melting curve of Fe using theoretical methods based on the formulation of quantum mechanics known as density-functional theory (DFT). Using DFT, we computed the free energy of solid (G_s) and liquid (G_l) Fe and obtained the melting curve as the locus of points in (p,T) space defined by the relation $G_l(p,T)=G_s(p,T)$.[13–15] The other theoretical works used DFT to fit classical potentials and then computed the melting curves of these classical potentials.[16,17]

Although we argued that the DFT melting curve of Fe should be reliable, especially at the pressure of the ICB, we recognize that the lack of solid experimental data makes it

difficult to validate those early results,[13–15] particularly in light of the fact that the practical use of DFT requires the introduction of an uncontrolled approximation, the exchange-correlation (XC) functional.

Here we try to prepare the ground to go beyond those early DFT calculations by setting the stage for the application of a much more accurate quantum mechanics technique, namely, quantum Monte Carlo (QMC). In particular, as a preliminary step toward the QMC calculation of the melting point of Fe at ICB pressure, we report the calculation of the room-temperature equation of state of hcp Fe from 0 to 400 GPa. Previous DFT calculations[3,4] using the generalized gradient approximation (GGA) corrections known as PW91 (Ref. 24) for the XC energy were in good agreement with experimental data, so we would not expect a worsening of these results with the current use of QMC. In fact, QMC has recently been successfully used to compute equation of states of a number of materials, including insulators such as MgO, MgH_2, and diamond,[25–28] semiconductor Si,[29] metals such as Mg (Ref. 27) and Al,[30] transition-metal oxide such as FeO,[31] and even the noble gas Ne.[32] In most of these cases the calculated structural parameters and the cohesive energy were in very good agreement with the available experimental data, where the latter is usually very difficult to obtain with DFT techniques.

This paper is organized as follows. In Sec. II we provide a brief description of QMC and the technical details used in our calculations. Finite-size effects are discussed in more detail in Sec. III. Section IV contains the main results and the equation of state of hcp Fe. Finally, in Sec. V we report the main conclusions of the work.

II. TECHNICAL DETAILS

Quantum Monte Carlo techniques have been described at length in previous papers,[33,34] so here we briefly review only the main issues relevant to our calculations. The most popular implementations of QMC are the variational Monte Carlo (VMC) method and the diffusion Monte Carlo (DMC) method. The former is a stochastic way to evaluate integrals, in particular the expectation value of the Hamiltonian of the system. The latter is a stochastic method to solve the Schrödinger equation in imaginary time. DMC is an exact method to project out the ground state of the system in the limit of long imaginary time; however, when dealing with fermions such as the electrons of a collection of atoms, practical calculations require the introduction of two approximations. The first is related to the antisymmetry of the wave function, which divides the space into adjacent pockets where the wave function changes sign, with these pockets being separated by the nodal surface. The presence of a nodal surface represents a problem for the stochastic evolution of the Schrödinger equation, the solution of which is usually presented in terms of the so-called fixed-node approximation (FNA),[33,35–38] in which the nodal surface is fixed to that of a known trial wave function, which is provided at the outset of calculations. The FNA represents a constraint, and because of this the DMC energy becomes only an upper bound to the true ground-state energy of the system. The second approximation is due to the need of replacing the Coulomb potential generated by the nuclei of heavy atoms with a pseudopotential, and in particular, by the introduction of the so-called locality approximation[39] to deal with the presence of nonlocal pseudopotentials. The locality approximation introduces an uncontrollable error, with respect to which the DMC energy is nonvariational. An alternative method to deal with nonlocal pseudopotentials in a consistent variational scheme was recently proposed by Casula.[40] DMC calculations with the FNA and the locality approximations become exact if the trial wave function is exact, and the errors in the DMC energy due to both approximations grows only quadratically with an error in the trial wave function.

It is generally believed, and indeed shown in a number of cases as mentioned in Sec. I, that despite the FNA and the locality approximation, DMC is much more accurate than DFT with the current XC functionals; however, it is also 10^3-10^4 times more expensive, and for this reason DMC applications are not yet numerous. This is of course set to change, thanks to the availability of faster and faster computers and in particular to the fact that QMC techniques adapt naturally to massively parallel computers.

The trial wave functions used in this work are of the Jastrow-Slater-type,

$$\Psi_T(\mathbf{R}) = e^{J(\mathbf{R})} D^{\uparrow}(\mathbf{R}) D^{\downarrow}(\mathbf{R}). \tag{1}$$

The $e^{J(\mathbf{R})}$ term in Eq. (1) is the so-called Jastrow factor and describes the electron-electron and electron-nucleus correlations ensuring that the cusp conditions are satisfied. Parameters appearing in this term are optimized using VMC by minimizing the variance of the local energy, $E_L(\mathbf{R}) = \Psi_T^{-1}(\mathbf{R}) H \Psi_T(\mathbf{R})$, where H is the Hamiltonian of the system and $\mathbf{R}$ represents the collections of the coordinates of all the electrons in the system. The terms $D^{\uparrow}(\mathbf{R})$ and $D^{\downarrow}(\mathbf{R})$ are Slater determinants of spin-up and spin-down single-electron orbitals. These Slater determinants set the nodal surface and ensure that $\Psi_T(\mathbf{R})$ is antisymmetric with respect to the swapping of the coordinates of any two electrons with the same spin.

The single-particle orbitals were obtained by plane-wave DFT calculations using the PWSCF (Ref. 41) code. We used a plane-wave cutoff of 75 hartree and re-expanded the single-particle orbitals in systematically improvable B splines[29] using a grid spacing given by $a = \frac{2}{3}\pi / G_{\max}$, where $G_{\max}$ is the length of the largest vector employed in the PW calculations, i.e., a grid 1.5 times finer than what is commonly referred to as the "natural" grid spacing.

Single-particle orbitals were initially produced with different XC functionals. We used the local-density approximation (LDA) (Ref. 42) and the PBE,[43] the hybrids B3LYP (Refs. 44 and 45) and PBE0,[46] and also the Hartree-Fock (HF) calculations. The calculated VMC and DMC energies and their variances are reported in Table I for a hcp Fe crystal containing two atoms with a volume of 8 Å^3/atom. The B3LYP functional provides one of the lowest variances and also the lowest DMC energy, and as a result we decided to use this functional to build up our trial wave functions for the rest of the work. All single-particle orbitals were constructed

TABLE I. VMC and DMC energies per atom (hartree units) for hexagonal closed packed iron at $V=8$ Å^3/atom, calculated with trial wave functions obtained from DFT with the LDA, PBE, B3LYP, and PBE0 functionals and with HF calculations. All single-particle orbitals were obtained using the plane-wave code PWSCF, with a plane-wave cutoff energy of 75 hartree and expanded in B splines with a grid spacing 1.5 times finer than the natural one (see text). Also reported is the variance of the VMC calculations.

	VMC		DMC
Model	E/atom (hartree)	Variance/atom (hartree^2)	E/atom (hartree)
PBE	−122.2722(4)	2.99(1)	−122.4789(2)
LDA	−122.2608(4)	3.14(1)	−122.4738(2)
HF	−122.3427(4)	2.53(1)	−122.4854(2)
B3LYP	−122.3385(4)	2.61(1)	−122.4964(2)
PBE0	−122.3353(4)	2.72(2)	−122.4963(2)

using a single zone-boundary point [the point (1/2, 1/2, 1/2) in lattice vectors units] in the Brillouin zone of the corresponding supercell.

We used the usual short-time approximation to evolve the Schrödinger equation in imaginary time. We tested different time steps, ranging from 0.0003 to 0.02 a.u, and repeating calculations on simulation cells containing two atoms at three different volumes $V=6.5$, 7.5, and 8 Å^3/atom. The conclusion from these tests was that using a time step of 0.01 a.u. gives rise to a volume-independent error, and therefore this is what we chose to use. All present calculations were performed using the CASINO code.[47]

III. FINITE-SIZE CORRECTIONS

Since QMC is a many-body theory, calculations on periodic systems need to ensure that the simulation cell is big enough so that electron-electron correlations have decayed away. However, periodicity also brings the additional problem that the true Coulomb interaction between the electrons has to be replaced by the Ewald interaction, which makes the QMC energy depend strongly on the size of the simulation cell. The problem comes from the interaction between the electrons and their exchange-correlation holes, which instead of having the correct $1/r$ behavior is replaced by a periodic interaction. For solids, this error can be shown to have a leading term which is inversely proportional to the volume of the system. This problem has been addressed in the past by various authors.[48–53] The solution of Fraser *et al.*[50–52] was to replace the Ewald interaction with a model periodic Coulomb (MPC) potential, which maintains the correct Ewald interaction for the evaluation of the Hartree energy but uses a periodically repeated potential based on the $1/r$ form for the interactions between the electrons and their exchange-correlation holes. The method of Chiesa, Ceperley, Martin, and Holzmann (CCMH) (Ref. 48) was based on the assumption that the correlation factor does not depend on the size of the simulation cell, and therefore the dominant finite-size errors on the potential and the kinetic energy are integration errors. These errors can be estimated from the behavior of the charge structure factor and from the Jastrow factor at low k vector, which can be calculated within a QMC simulation using highly accurate trial wave functions. These two methods address the problem of the so-called two-body finite-size corrections. Once these two-body corrections are taken into account, there is an additional one-body-like correction equivalent to the **k**-point sampling error in single-particle calculations such as DFT. This one-body correction can be estimated using standard DFT. Recently, Kwee, Zhang, and Krakauer (KZK) (Ref. 49) proposed to compute the two-body corrections in a very simple way. They suggested to correct the QMC calculations with a finite-size DFT-LDA calculation, in which the standard LDA XC energy is replaced by a finite-size LDA energy, computed with the same supercell used in the QMC calculations. To do this, they repeated the early calculations of Ceperley and Alder[54] for the homogeneous electron gas at a series of values for the electron density and for different volumes. The standard LDA functional is obtained by extrapolating these results to infinite size, but Kwee *et al.*[49] produced a family of functionals, which depend on the number of electrons (or the volume) of the system. They showed that the method works very well for bulk silicon, and it is extremely simple; it does not require any modification of the QMC code as it is a postprocessing correction, and as such is much more straightforward to apply. Kwee *et al.*[49] only developed their corrections for cubic cells; however, they showed that their method worked equally well also for noncubic systems. Here we reinforce their findings by showing that the method works well also for hexagonal closed packed iron. One of us has implemented the KZK method in the PWSCF code, and here we show results obtained both with the KZK and the CCMH methods.

We should note that the KZK correction is expected to work well in systems where DFT LDA performs reasonably well, similar to metallic iron in the present case or bulk silicon in the original work of Kwee *et al.*[49] However, for strongly correlated systems such as Mott insulators the DFT-LDA performance can be poor, so it is not clear if in those systems the KZK correction might perform equally well. The CCMH method is based on the structure factor calculated within DMC, and therefore should have a wider range of applicability.

In Fig. 1 we show DMC calculations for cells containing 8, 36, 54, 64, 96, and 150 atoms at two different volumes, $V=7$ and 8 Å^3/atom. As mentioned in Sec. II, most DMC simulations were run for at least 5000 steps, but the calculations with 150 atoms were only run for 1000 steps due to their very large cost, so we put less weight on the results obtained with this cell size, which we only show for completeness. Besides the raw DMC data, we also show DMC +one-body corrections and DMC+one-body+two-body corrections, with the two-body terms computed using KZK and CCMH. It is clear that both the KZK and the CCMH methods work equally well. More importantly, since we are interested in the EOS, the relevant physical quantities of interest are relative energies, which are expected to converge to infinite size earlier than absolute energies. In Fig. 1 we show the differences between the DMC energies at $V=7$ and

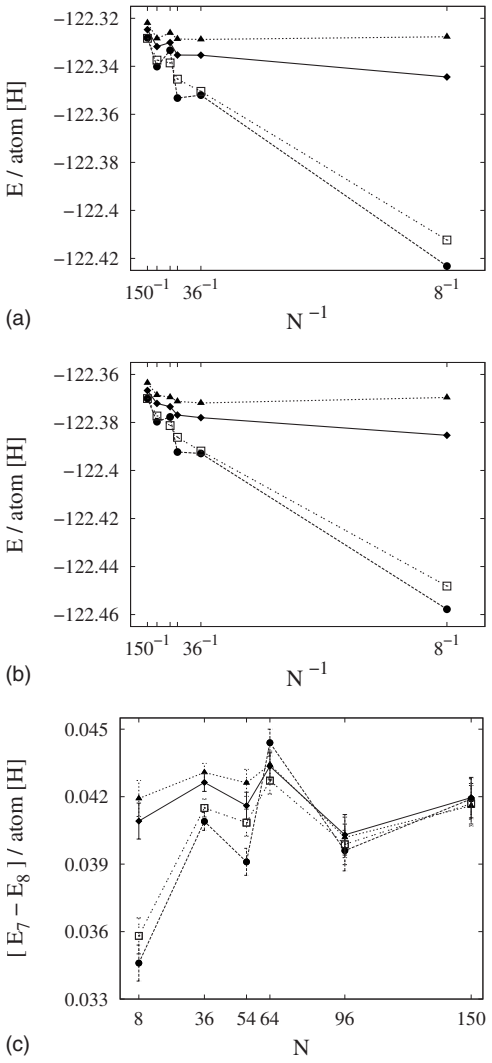

FIG. 1. Finite-size-corrected DMC energies (in units of hartree/atom) for various simulation cell sizes. Curves show the uncorrected DMC energy (circles—dashed line), DMC+one-body corrections (open square—double point line), and DMC+one-body +two-body corrections using CCMH (triangle—points line) and KZK (diamonds—solid line). Top and central figures report calculations at volumes $V=7$ and 8 Å^3/atom, respectively. Bottom figure shows energy differences between the two volumes.

8 Å^3/atom, and we can see that once both one-body and two-body corrections are introduced finite-size effects are very small. In fact, there is not much to be gained by using cells containing more than 36 atoms, and even 8 atoms seem to be enough. However, we decided to use cells containing 36 atoms for the rest of the calculations.

IV. EQUATION OF STATE OF hcp Fe

We performed nine DMC calculations with volume between 6.25 and 11 Å^3/atom, covering the range of pressures relevant to Earth's core. Each value has been calculated using 1280 walkers and 5000 DMC steps, ensuring in all cases that the local energy was well behaved. With these choices, all energies were obtained with errors of ~0.6 mhartree/atom (one standard deviation).

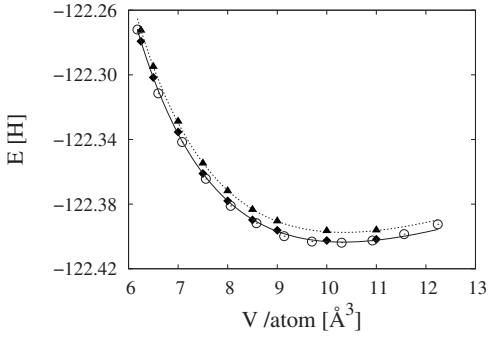

FIG. 2. DMC energies (in hartree units) as a function of volume corrected using both the CMMH (triangles—points line) and the KZK (diamonds—solid line) schemes. Data also include quasiharmonic Helmholtz free energies at 298 K computed with DFT PW91 (Refs. 15 and 55). The curves through the points are fits to Birch-Murnaghan equation of states. DFT-PW91 data from Ref. 3 (open circles) are also reported for comparison.

Each DMC value presented in this section has been obtained using 128 computers in parallel. Around 1000 s are necessary to evolve all the walkers 20 Monte Carlo time steps on a Cray-XT4 machine.

Hexagonal closed packed Fe has an additional degree of freedom, which is the value of the ratio between the lattice vector perpendicular to the basal plane and one of the lattice vectors in the basal plane, the c/a ratio. Using DFT PBE, we explored the dependence of the energy with respect to c/a at different volumes and found that the optimal c/a varies between 1.54 and 1.60 in the range of volumes investigated here. However, by taking the constant value $c/a=1.57$, we found that the equation of state is essentially unchanged, and therefore all our DMC calculations were performed with this choice of c/a.

Since the available experimental data for the EOS of Fe have been taken at room temperature, we added on the calculated DMC energies the free energies calculated at 298 K using quasiharmonic calculations performed with DFT.[15,55] Room-temperature thermal expansion is small but it reaches almost 3 GPa at a pressure of 300 GPa, so it is not completely negligible.

Figure 2 shows these room-temperature DMC free energies for different volumes, both using the KZK and the CCMH finite-size corrections, together with a fit to a third-order Birch-Murnaghan equation.[56] There is a small energy shift between the KZK and the CCMH corrected DMC results, but this shift is essentially constant throughout the entire volume range, and therefore does not affect the pressure and structural properties such as the equilibrium lattice parameter and the zero pressure bulk modulus. For comparison, we also plot the earlier DFT-PW91 results of Söderlind *et al.*,[3] offset by a constant for convenience and corrected with the same room-temperature quasiharmonic free energies. It is clear that these early DFT results and the present DMC results are very similar, so it is not surprising that the pressure versus volume curves are also very similar. These are plotted in Fig. 3, where the statistical errors associated with the parameters of the Birch-Murnaghan fit are responsible for a band error of the DMC pressure vs volume curve. As the

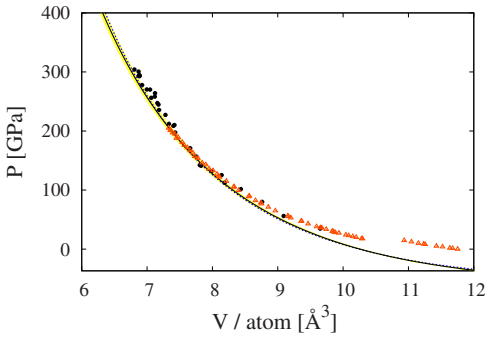

FIG. 3. (Color online) Pressure vs volume curve obtained from DMC calculations corrected for finite-size effects using the KZK scheme (solid line). Results obtained using the CMMH scheme are indistinguishable and therefore not reported. The error band in the DMC curve is due to the errors in the parameters of Birch-Murnaghan fit. DFT-PW91 results (Ref. 3) (dotted line) and experimental data [circles (Ref. 1) and open triangles (Ref. 2)] are also reported for comparison. Notice the discontinuity due to the hcp-bcc phase transition in the values provided by Dewaele *et al.* (Ref. 2). At low pressures, calculations and experiments differ because of the magnetism, which is not taken into account in the present results.

figure shows, the DMC equation of state in the high-pressure region of the phase diagram agrees closely with the experiments carried out by Mao *et al.*[1] and Dewaele *et al.*,[2] as well as with the DFT-PW91 calculations.[3] The discontinuity in the results of Dewaele *et al.*[2] was due to the hexagonal close packed to body-centered-cubic phase transition in solid iron around ~10 GPa. The agreement between the calculations and the experiments worsens at low pressure due to the onset of magnetism which is not taken into account in the present calculations;[57] however, for present and future purposes our concern confines to high pressure, in which the agreement between our calculations and the experiments is indeed very good.

V. CONCLUSIONS

We have calculated the equation of state of iron in the hexagonal closed packed structure up to pressures relevant to Earth's core using highly accurate diffusion Monte Carlo techniques. We showed that the recently proposed treatment of finite-size effects in quantum Monte Carlo by Kwee *et al.*[49] is very efficient and easy to use compared to more sophisticated schemes developed in the past few years,[48,50] and a direct comparison with the scheme developed by Chiesa *et al.*[48] has confirmed this. Our calculations employed pseudopotentials with the locality approximation and the standard fixed-node approximation. The calculated equation of state in the high-pressure region of the phase diagram is found to be in good agreement with the available experimental data,[1,2] and therefore lends support to the reliability of DMC techniques on this system. This work establishes the basis for future developments aimed at the calculation of high-temperature properties of iron, and in particular its melting temperature at inner-core boundary condition, which will be reported in due course.

ACKNOWLEDGMENTS

The computations were performed on the HECToR service, using allocations of time from an EPSRC "Capability challange" grant. The work of E.S. was supported by NERC.

[1] K. Mao, Y. Wu, L. C. Chen, and J. F. Shu, J. Geophys. Res. **95**, 21737 (1990).
[2] A. Dewaele, P. Loubeyre, F. Occelli, M. Mezouar, P. I. Dorogokupets, and M. Torrent, Phys. Rev. Lett. **97**, 215504 (2006).
[3] P. Söderlind, J. A. Moriarty, and J. M. Wills, Phys. Rev. B **53**, 14063 (1996).
[4] D. Alfè, G. Kresse, and M. J. Gillan, Phys. Rev. B **61**, 132 (2000).
[5] Q. Williams, R. Jeanloz, J. D. Bass, B. Svendesen, and T. J. Ahrens, Science **236**, 181 (1987).
[6] R. Boehler, Nature (London) **363**, 534 (1993).
[7] G. Shen, H. Mao, R. J. Hemley, T. S. Duffy, and M. L. Rivers, Geophys. Res. Lett. **25**, 373 (1998).
[8] Y. Ma, M. Somayazulu, G. Shen, H. K. Mao, J. Shu, and R. Hemley, Phys. Earth Planet. Inter. **143**, 455 (2004).
[9] J. M. Brown and R. G. McQueen, J. Geophys. Res. **91**, 7485 (1986).
[10] J. H. Nguyen and N. C. Holmes, Nature (London) **427**, 339 (2004).
[11] L. R. Benedetti, N. Guignot, and D. L. Farber, J. Appl. Phys. **101**, 013109 (2007).
[12] D. Alfè, G. D. Price, and M. J. Gillan, J. Phys. Chem. Solids **65**, 1573 (2004).
[13] D. Alfè, M. J. Gillan, and G. D. Price, Nature (London) **401**, 462 (1999).
[14] D. Alfè, G. D. Price, and M. J. Gillan, Phys. Rev. B **65**, 165118 (2002).
[15] D. Alfè, G. D. Price, and M. J. Gillan, Phys. Rev. B **64**, 045123 (2001).
[16] A. B. Belonoshko, R. Ahuja, and B. Johansson, Phys. Rev. Lett. **84**, 3638 (2000).
[17] A. Laio, S. Bernard, G. L. Chiarotti, S. Scandolo, and E. Tosatti, Science **287**, 1027 (2000).
[18] C. M. S. Gannarelli, D. Alfè, and G. M. J., Phys. Earth Planet. Inter. **152**, 67 (2005).
[19] L. Vočadlo, J. Brodholt, D. Alfè, G. D. Price, and M. J. Gillan, Geophys. Res. Lett. **26**, 1231 (1999).
[20] L. Vočadlo, D. Alfè, M. J. Gillan, and G. D. Price, Phys. Earth Planet. Inter. **140**, 101 (2003).
[21] L. Vočadlo, D. Alfè, M. J. Gillan, I. G. Wood, J. P. Brodholt, and G. D. Price, Nature (London) **424**, 536 (2003).
[22] H. K. Mao *et al.*, Science **292**, 914 (2001).
[23] J.-P. Poirier, *Introduction to the Physics of the Earth's Interior* (Cambridge University Press, Cambridge, England, 1991).
[24] J. P. Perdew, J. A. Chevary, S. H. Vosko, K. A. Jackson, M. R. Pederson, D. J. Singh, and C. Fiolhais, Phys. Rev. B **46**, 6671

(1992).
[25] D. Alfè, M. Alfredsson, J. Brodholt, M. J. Gillian, M. D. Towler, and R. J. Needs, Phys. Rev. B **72**, 014114 (2005).
[26] D. Alfè and M. J. Gillan, J. Phys.: Condens. Matter **18**, L435 (2006).
[27] M. Pozzo and D. Alfè, Phys. Rev. B **77**, 104103 (2008).
[28] R. Maezono, A. Ma, M. D. Towler, and R. J. Needs, Phys. Rev. Lett. **98**, 025701 (2007).
[29] D. Alfè and M. J. Gillan, Phys. Rev. B **70**, 161101(R) (2004).
[30] R. Gaudoin, W. M. C. Foulkes, and G. Rajagopal, J. Phys.: Condens. Matter **14**, 8787 (2002).
[31] J. Kolorenč and L. Mitas, Phys. Rev. Lett. **101**, 185502 (2008).
[32] N. D. Drummond and R. J. Needs, Phys. Rev. B **73**, 024107 (2006).
[33] W. M. C. Foulkes, L. Mitas, R. J. Needs, and G. Rajagopal, Rev. Mod. Phys. **73**, 33 (2001).
[34] C. J. Umrigar, M. P. Nightingale, and K. J. Runge, J. Chem. Phys. **99**, 2865 (1993).
[35] J. B. Anderson, J. Chem. Phys. **63**, 1499 (1975).
[36] J. B. Anderson, J. Chem. Phys. **65**, 4121 (1976).
[37] J. W. Moskowitz, K. E. Schmidt, M. A. Lee, and M. H. Kalos, J. Chem. Phys. **77**, 349 (1982).
[38] P. J. Reynolds, D. M. Ceperley, B. J. Alder, and W. A. Lester, Jr., J. Chem. Phys. **77**, 5593 (1982).
[39] L. Mitáš, E. L. Shirley, and D. M. Ceperley, J. Chem. Phys. **95**, 3467 (1991).
[40] M. Casula, Phys. Rev. B **74**, 161102(R) (2006).
[41] S. Baroni, A. Dal Corso, S. de Gironcoli, and P. Giannozzi, http://www.pwscf.org
[42] W. Kohn and L. J. Sham, Phys. Rev. **140**, A1133 (1965).
[43] J. P. Perdew, K. Burke, and M. Ernzerhof, Phys. Rev. Lett. **77**, 3865 (1996).
[44] K. Kim and K. D. Jordan, J. Phys. Chem. **98**, 10089 (1994).
[45] P. J. Stephens, F. J. Devlin, C. F. Chabalowsky, and M. J. Frisch, J. Phys. Chem. **98**, 11623 (1994).
[46] C. Adamo and V. Barone, J. Chem. Phys. **110**, 6158 (1999).
[47] R. J. Needs, M. D. Towler, N. D. Drummond, and P. López Ríos, *CASINO Version 2.1 User Manual* (University of Cambridge, Cambridge, England, 2007).
[48] S. Chiesa, D. M. Ceperley, R. M. Martin, and M. Holzmann, Phys. Rev. Lett. **97**, 076404 (2006).
[49] H. Kwee, S. Zhang, and H. Krakauer, Phys. Rev. Lett. **100**, 126404 (2008).
[50] L. M. Fraser, W. M. C. Foulkes, G. Rajagopal, R. J. Needs, S. D. Kenny, and A. J. Williamson, Phys. Rev. B **53**, 1814 (1996).
[51] A. J. Williamson, G. Rajagopal, R. J. Needs, L. M. Fraser, W. M. C. Foulkes, Y. Wang, and M.-Y. Chou, Phys. Rev. B **55**, R4851 (1997).
[52] P. R. C. Kent, R. Q. Hood, A. J. Williamson, R. J. Needs, W. M. C. Foulkes, and G. Rajagopal, Phys. Rev. B **59**, 1917 (1999).
[53] N. D. Drummond, R. J. Needs, A. Sorouri, and W. M. C. Foulkes, Phys. Rev. B **78**, 125106 (2008).
[54] D. M. Ceperley and B. J. Alder, Phys. Rev. Lett. **45**, 566 (1980).
[55] D. Alfè, computer code PHON, UCL, London, 1998, http://www.chianti.geol.ucl.ac.uk/dario
[56] F. Birch, Phys. Rev. **71**, 809 (1947).
[57] G. Steinle-Neumann, L. Stixrude, and R. E. Cohen, Proc. Natl. Acad. Sci. U.S.A. **101**, 33 (2004).